Electrical Power and Energy Systems 143 (2022) 108436

Contents lists available at ScienceDirect

International Journal of Electrical Power and Energy Systems

journal homepage: www.elsevier.com/locate/ijepes

Distributed Model Predictive Control for voltage coordination of large-scale wind power plants

César Contreras [a], Alicia Triviño [b,*], José A. Aguado [b]

[a] Decanato de Investigacion, Universidad Nacional Experimental del Tachira (UNET), San Cristobal, 5001, Venezuela
[b] Department of Electrical Engineering, Escuela de Ingenierias Industriales, University of Malaga, Malaga, 29010, Spain

ARTICLE INFO

Keywords:
Distributed
Model predictive control
STATCOM
Wind power plants

ABSTRACT

This paper presents a Distributed Model Predictive Control (DMPC)-based algorithm for distributed and coordinated voltage control of wind power plants. Under the proposed approach, voltage magnitude at the point of connection of wind power plants is optimally controlled to meet voltage requirements. In a conventional centralized approach, each wind power farm tracks the control signals set by the Transmission System Operator but DMPC responds locally to mitigate the voltage deviations without the central commands. The problem is cast as one of optimal control, which is solved at every time step by a distributed optimization. A dual decomposition scheme is proposed to solve the distributed optimization problem where the voltages magnitude of the common nodes are used as a consensus term for the coordination. In order to extend the applicability of this control, the proposed DMPC is carefully designed in such a way that it does not require any change in the inner control of the electrical machines, controls or compensators. The algorithm has been tested on an IEEE 9-bus system with two wind power plants and on an IEEE 14-bus system with three power plants. In both cases, the plants are not directly connected. Following an analysis of the achievable performance and the computational resources consumed by the local algorithm, the results of the simulations confirm that the proposed control approach is suitable for the voltage coordination of wind power plants with acceptable scalable results.

1. Introduction

Renewable energy sources are now a common asset in power systems in the form of small generators (distributed generation — DG) or even connected to transmission networks. Wind power generation has demonstrated its economic feasibility for both configurations. The penetration of wind energy is expected to have a projected growth from 2021 through 2028 of up to 90 GW [1]. As a result, wind farms will have a significant impact on the power system. Currently, modern wind farms incorporate a voltage and reactive power control system to regulate the voltage at the Point of Connection (POC). They thus keep the voltages within a specific range to mitigate the negative effects caused by intermittent wind power [2]. For voltage regulation, the most effective variable to consider is the reactive power, which leads to the volt/var control. As described in [3], several challenges should be addressed to cope with some particularities involved in the volt/var operation of large wind farms due to their intermittent nature. Based on this fact, many countries have developed specific grid codes for wind farms, which stipulate that these installations should contribute to voltage control of the power systems.

Therefore, it is critical to develop algorithms and methods for this control, which make it easier to integrate these systems in the grid. To that end, it is common to use voltage compensators, such as the Static Synchronous Compensator (STATCOM) in order to comply with the grid codes offering a secondary voltage control. These can be integrated into the machine controllers or built as an additional controller for a set of wind turbines, referred to as a wind farm [4] or a wind power plant. The common topology for a wind farm is shown in Fig. 1 [5].

Although wind power plants have their own local control to operate the controller, it is necessary to coordinate these large-scale generation units to establish an effective control voltage while minimizing generation curtailment [6]. The works in [7–9] focus on how to perform the voltage control among the elements of only one wind farm. A more ambitious approach with a higher impact on the grid would be the definition of voltage control for several wind farms.

Thus, to achieve an adequate and safe power system voltage control, there needs to be adequate control and coordination of the reactive power compensators of several wind farms. In a transmission network, the Transmission System Operator (TSO) is in charge of coordinating

* Corresponding author.
E-mail address: atc@uma.es (A. Triviño).

https://doi.org/10.1016/j.ijepes.2022.108436
Received 28 December 2021; Received in revised form 22 May 2022; Accepted 15 June 2022
Available online 30 June 2022

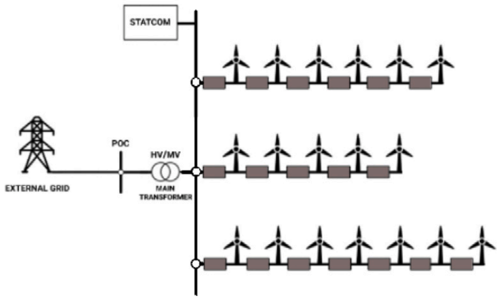

Fig. 1. Diagram of a common controller for a wind power plant.

different reactive sources (mainly synchronous generators and compensation units) to ensure the reactive power balance of the entire system. Thus, one of the goals of this operator should be to adjust the optimal set point (SP) of the local controllers, incorporating knowledge of the environment or market platform. To do so, the TSO gathers all the information about the components in the network. It then analyses the data and usually solves an optimization problem in order to decide the SP of the local controllers. The SPs are sent to the controlled units as seen in Fig. 2. This is a centralized voltage control strategy, which can achieve an optimal control performance by processing the overall information if the data are precise and not manipulated intentionally or by a transmission error. However, centralized approaches might not be suitable for a future scenario with multiple large-scale wind farms. As described in [10], centralized voltage controllers are associated with significant computational costs, which are driven by the need for global and complete data. The optimization-based methods designed in these approaches are usually executed in a period of several seconds or even minutes with a slow response time. Hence, they might not be able to handle short-term voltage [5]. The need for substantial computational resources and the increased execution time with the number of controllable units limit the scalability of the centralized solutions. Moreover, they lack robustness and reliability due to potentially inaccessible data. As power systems constitute a critical infrastructure, it is necessary to take into account the threats that their operation entitles. As explained in [11], false data injection or man-in-the middle are common threats with which these systems must cope.

In order to offer more robust solutions and to shorten the response times, distributed approaches have been proposed in recent years as strategies that get a performance close to the centralized algorithm but with added capabilities as scalability, enhanced cyber-security. They also perform better than centralized solutions when there is data unavailability [12]. The simplest and most cost-efficient methods follow a distributed and autonomous approach (usually referred to as decentralized) in which the nodes reconfigure their own voltages without coordinating with any other nodes in the network. This could lead to impractical solutions which do not comply with the electrical restrictions imposed by the power system. This strategy is enhanced when partial information about the network state is considered, leading to distributed algorithms. In the context studied, a compensator could make use of the information sent by its immediate neighbours in the grid topology, and of some common buses with a high impact on the performance of the nodes where the compensators are placed. With a distributed control, these partial data are incorporated into the controllers' own sub-problems. In order to reach the optimum solution (such as that provided in the centralized approach), an iterative process must be executed. There are therefore three main benefits of using a correctly designed, coordinated and distributed architecture when compared with a centralized approach. Firstly, communication costs and delays are minimized. Secondly, the input data in the controller is reduced so that a faster response may be achieved when solving the problem, which could even be solved more frequently. The computational time of this local algorithm is lower than that associated with the centralized approach. Moreover, it is less dependent on the number of units that need to be controlled, so scalability can be fulfilled with distributed approaches [13]. Finally, it can be adjusted to data unavailability due to privacy concerns or technical problems in the infrastructure. The vulnerabilities in this control are also restricted to a smaller area, which may help to incorporate cybersecure protection and monitoring techniques.

Model Predictive Control (MPC) can be applied to distributed voltage controls. The basis of this algorithm consists in repeatedly solving a multi-time-step constrained optimization problem with a sensitivity model to predict the system evolution. The MPC captures the dynamics of the system over a time horizon and resolving an optimization algorithm, the best control setting is determined adding control stability. Unlike conventional control strategies focusing on exploring the closed-loop control law, the MPC transforms the control problem into an online open-loop optimization problem by building discrete mathematical models and cost functions. When implemented in a distributed way, the stable and efficient operation of networks is achieved as in [14], which illustrates its application to a power system with distributed generation. In this work, the control algorithm is embedded within the voltage and reactive power controller. Using the dynamics of the primary control, they model the dynamics of the state variable that is used in the predictive control. The formulation of the distributed MPC (DMPC) presented in [15] also relies on the machine features to decide the parameters used to configure the DG units. Specifically, the authors consider wind turbines in their analysis.

In order for this control to be applied more extensively, the controller we propose is carefully designed so that it does not require any change in the compensators and does not rely on the specific model of the controlled machine. In fact, it will follow a plug-and-play structure in which the new controller is inserted into any machine operated with an SP, as shown in Fig. 2. This incorporation is accomplished seamlessly by modifying the SP (initially transmitted by the TSO in a centralized approach). It is worth noting that the proposed controller is valid for any type of large-scale generation unit (i.e. wind or solar farm) or device with a local voltage controller due to these inherent properties. As the machine dynamics are not considered for the DMPC, the proposed control can be applied in any machine/device which has a local voltage control with an accessible input for the setpoint. This plug-and-play control reduces the technical and economic costs of the implementation, which also provides a scalable solution. To illustrate this idea, the diagram in Fig. 2 shows a system with generators connected on buses 1, 2 and 5. Buses 2 and 5 are connection buses of alternative generation sources with voltage compensators and their respective controls. Loads are located on buses 3 and 6. Without applying our proposed algorithm, the STATCOMs would be configured by the TSO. This unit would specify the setpoints Vsp_1 and Vsp_2 for STATCOMs in buses 2 and 5 respectively. Our proposal does not change the electronics or the internal control of the STATCOM or the renewable farm. A DMPC is inserted for each compensator control to locally determine the new setpoint without making structural alterations or relying on internal parameters of the machine or the compensator. The control already installed in each STATCOM is operated solely with a new input, which corresponds to the result of a DMPC algorithm. For this particular topology, bus 3 is common for both types of renewable energy farms, and we assume that it would be strongly impacted by buses 2 and 5 i.e. it would show a high sensitivity. Thus, we can coordinate the two compensators based on common bus variables as is shown in the input variables of the DMPC algorithm. Following a distributed approach, the algorithm we propose also estimates the value of the control setup of the other STATCOM in the previous iteration $\mu_2(k-1)$ and $\mu_1(k-1)$ in buses 1 and 5 respectively. This estimation is done from the value of the common variables $V_3^2(k)$ and $V_3^1(k)$, which are determined and published by each control in each iteration.

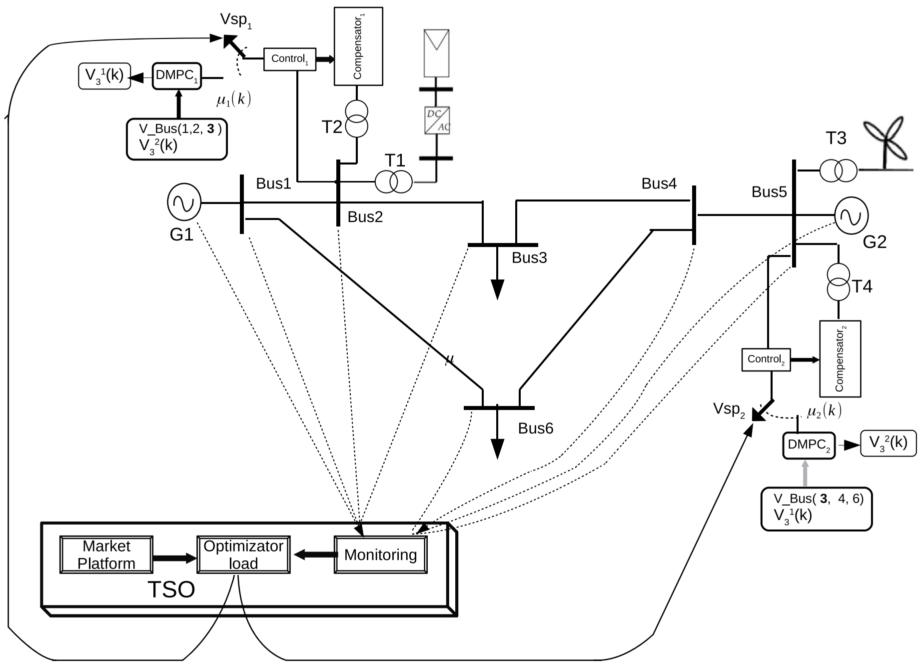

Fig. 2. Diagram of the proposed plug-and-play controller based on DMPC.

The control action μ of each controller is not exchanged because it is needed to increase the degree of autonomy for future events such as loss of communication, and to maintain privacy over the operation and control plan of each zone. We can observe that other nodes' information required by these local controllers comes from a small set of other DMPCs in the transmission network. In particular, only DMPCs that share a common bus must exchange this kind of information. The controls are executed periodically, and on each occasion they perform an iteration process. In each iteration, each DMPC solves an optimization problem that minimizes the deviation of the voltage values, the control action and the penalty on the difference of the negotiation variables of its zone. From the control action obtained in each iteration, each control calculates the deviation of the common bus trading variable and publishes it. These values are used to estimate the control action applied by the other DMPCs of influence. This value will be used in the next iteration. Each control then compares its negotiation variable with that of the other control. The process ends when the difference of the trading variables is below a threshold, or a certain number of iterations has been reached.

The main contributions of this work are:

- It proposes a fully distributed approach for the voltage control. It can be easily implemented in the original wind farm controllers. Moreover, it is compatible with most control algorithms proposed in the literature [7–9] to distribute the reactive power demand among the wind turbines of a wind farm. The distributed algorithm proposed uses the voltage of its immediate nodes and only exchanges information with a small set of other DMPCs in the grid (those that have a bus in common, on which they must reach a consensus). Each DMPC acts according to its predicted movements and the current information from these closed nodes.
- The original controllers of the compensators are therefore not modified in a plug-and-play scheme. In fact, the specific dynamic of the machine is not used for the DMPC but requires the network state instead. Thus, the proposed DMPC controller is valid for multiple types of large-scale generation units.
- The network topology is intrinsic to the design, allowing it to be considered in the controller's decisions. Specifically, by using this information, we detect the buses that have more influence on other nodes and we restrict the input data of the controller to the state of these influencing nodes. This approach minimizes the information that the DMPC units exchange, which can provide a clear advantage in terms of scalability and data security.

The rest of this paper is organized as follows. In Section 2, the control model is done first by determining the prediction model of the bus voltages from the decoupled power flow equations and separating the controllable buses from the non-controllable ones. Then, in Section 3, using Lagrangian techniques, decomposition is applied to the global MPC equation to obtain a local predictive control based on the distributed model. Section 4 applies the proposed distributed control to an IEEE 9-bus test system with two wind farms including their compensation with STATCOMs. The load profile has been varied to verify the effectiveness of the proposed controller. Finally, Section 5 presents the main conclusions and outlines some future research lines.

2. Related work

In general, most references focus on the control of active and reactive power and the voltage in the POC connection bus of a single wind farm composed of multiple turbines. The values of the variables of these buses in some cases are taken to execute a consensus as in [4,13]. The consensus via critical buses, which can be identified as in [13], requires some communication channel to transmit the state of the buses. This constitutes a vulnerability, which could be avoided considering other buses. Other algorithms like in [16,17] and the one proposed in this work, they do consider different wind farms connected at different points of the network. In [16], the authors determine a critical bus to execute the consensus. In [17], the proposed algorithm does not require consensus but they achieve coordination by an iterative algorithm to configure two λ values. These values depend on the voltage deviation of the buses to which the distributed generation units are connected and the power losses. Although the algorithm can be solved locally, it requires the information of all the voltage deviations, which needs a communication network and it prevents scalability. In our proposed algorithm, a common bus is chosen based on the maximum sensitivity value between each POC bus and the network buses. This is an advantage because a consensus is executed on the basis of real electrical

Table 1
Comparison of algorithms.

Reference	Testing system	Wind farms	Algorithm	Consensus bus	Neighbouring buses	Plug and play
[4]	IEEE9	1	MPC	POC	✗	✗
[13]	IEEE14	1	DMPC	POC	✗	✓
[16]	IEEE14	Several	MPC	Critical bus	✗	✓
[17]	Hami region of Xinjiang	Several	Genetic algorithms	✗	✗	✓
Proposed control	IEEE9 IEEE14	Several	DMPC	✓	✓	✓

connections instead of using a communication network as in [13,16]. Finally, as can be seen in Table 1, the most resulting advantage of our proposed algorithm is that it includes neighbouring buses. This guarantees that the largest number of buses in the network remains within the voltage profile set by the code requirements of the system operator. In addition, as there is not a new communication network to install and knowing the machine dynamics is not a requirement, it is a simpler algorithm to implement since it does not involve noticeable modifications of the equipment.

3. Problem formulation

It is well known that most power grids with multiple nodes can be described by a linear model close to an operating point S_0 or desired state. This behaviour is defined by Eq. (1), where ΔP is the difference vector of active power of nodes with respect to those in the operating point, ΔQ is the difference vector of the reactive power in the aforementioned states, V represents the voltage magnitude in the nodes and δ is their voltage angles [18]. For well-conditioned problems, this matrix system can also be reduced to Eq. (2). This strategy is the decoupled power flow model which is based on an approximated version of the Jacobian matrix used in the Newton–Raphson method. This simplification is based on the fact that active power is much more sensitive to small changes in the phase angle at the node, and reactive power is more sensitive to small voltage changes.

$$\begin{bmatrix} \Delta P \\ \Delta Q \end{bmatrix} = \begin{bmatrix} \frac{\partial P}{\partial \delta} & \frac{\partial P}{\partial V} \\ \frac{\partial Q}{\partial \delta} & \frac{\partial Q}{\partial V} \end{bmatrix} \begin{bmatrix} \Delta \delta \\ \Delta |V| \end{bmatrix} \tag{1}$$

$$\begin{bmatrix} \Delta P \\ \Delta Q \end{bmatrix} = \begin{bmatrix} \frac{\partial P}{\partial \delta} & 0 \\ 0 & \frac{\partial Q}{\partial V} \end{bmatrix} \begin{bmatrix} \Delta \delta \\ \Delta |V| \end{bmatrix} \tag{2}$$

Considering that the line susceptances B are much larger than the line conductances, we can simplify the Jacobian matrix in the previous model leading to Eq. (3) for a power system with n nodes. As can be observed, the reactive power is related to the voltage magnitude using the decoupled power flow, in which B_{ij} is the susceptance in the line connecting node i to node j [19].

$$\begin{bmatrix} \Delta Q_1 \\ \vdots \\ \Delta Q_n \end{bmatrix} = - \begin{bmatrix} B_{11} & \dots & B_{1n} \\ \vdots & \ddots & \vdots \\ B_{n1} & \dots & B_{nn} \end{bmatrix} \begin{bmatrix} \Delta |V_1| \\ \vdots \\ \Delta |V_n| \end{bmatrix} \tag{3}$$

The decoupled power flow equations constitute an approximated but valid model of the power system that relates the change in the voltage magnitude or reactive power at any given bus to the change in the voltage magnitude or reactive power at the rest of the buses in the system. In other words, if a change occurs in one bus, we could infer the impact of this change on the other buses. This impact can be measured by the sensitivity and the electrical distance, as considered in [20–22].

Eq. (3) can be better detailed by separating it into controllable and non-controllable nodes as in [18], leaving the one expressed in (4).

$$\begin{bmatrix} \Delta Q_u(k) \\ \Delta Q_c(k) \end{bmatrix} = - \begin{bmatrix} B_{uu} & B_{uc} \\ B_{cu} & B_{cc} \end{bmatrix} \begin{bmatrix} \Delta |V_u(k)| \\ \Delta |V_c(k)| \end{bmatrix} \tag{4}$$

where the subscript c, u, and k are used to indicate controllable and non-controllable voltage nodes and the time instant respectively. The susceptance of the network is considered constant. Hence, the following equation can be considered:

$$[\Delta Q_u(k)] = -[B_{uc}][\Delta |V_c(k)|] - [B_{uu}][\Delta |V_u(k)|] \tag{5}$$

where $[\Delta Q_u(k)]$ is the vector of the reactive powers of the non-controllable nodes at the instant k, $[B_{uc}]$ is the matrix of the susceptances of the lines that connect the controllable and non-controllable nodes, $[B_{uu}]$ is the matrix of the susceptances of the lines connecting the non-controllable nodes and $\Delta |V_c(k)|$, $\Delta |V_u(k)|$ are the vectors of the voltages at the controllable and non-controllable nodes respectively at the instant k. It is also possible from (5) to obtain the expression below (Eq. (6)) with which the voltage of the non-controllable nodes at the instant $(k+1)$ can be calculated from the voltage of the controllable nodes at that same instant.

$$(\Delta |V_u(k+1)|) = -(B_{uu})^{-1}(\Delta Q_u(k)) - (B_{uu})^{-1}(B_{uc})(\Delta |V_c(k+1)|) \tag{6}$$

The Power Flow (PF) method is an iterative process in which a voltage value V is estimated and then the system of equations is solved with a method such as Newton–Raphson's. With this resolution, the values of Q and V are found so that the system of equations is fulfilled. ΔV obtained in each iteration is the voltage correction made to the estimated voltage value.

Considering the problem addressed in this paper, we have to take into account the fact that decomposition techniques for the optimization problem are used to solve and coordinate the voltage control of large areas with multiple generators. They have proven to be applicable in the design of DMPC for coordinating voltage compensation devices [23]. These same techniques are used to develop the controller proposed in this work.

When the control is applied to a voltage compensator, the previous formulation differs because the ΔV is the deviation from the desired voltage at the connection point, i.e. $\Delta V = V_{SP} - V_{measured}$, where V_{SP} is the setpoint value of the voltage (for example 1 pu) and $V_{measured}$ is the measured voltage value. With this in mind, the prediction model of the controller is then determined.

Eq. (6) illustrates how the ongoing reactive power $\Delta Q_u(k)$ disturbs uncontrolled voltage nodes at the next interval. If the ongoing disturbances are known, the new control action $\Delta V_c(k+1) = \mu(k)$ should then be applied. This voltage setpoint in the controlled nodes is expected to minimize the voltage deviation of the uncontrolled nodes in the near future, i.e. in $\Delta V_u(k+1)$. In other words, in each time step the ongoing voltage deviation is searched for in order to modify the setpoint of the controllable voltage nodes in successive time steps. $\Delta V_u(k)$, represents the deviation from the desired value of the voltage measured in the uncontrolled nodes, i.e. nodes without voltage controllers. Conversely, the $\Delta V_c(k)$ are the voltages of the nodes with local area controllers that already have their own measurement devices.

The obvious control strategy is to select a control action (change the setpoints of the controllable nodes) in order to minimize the voltage deviation of the other nodes ($\Delta V_u(k)$). Due to sensitivity, we find that the voltage variations are proportional to the reactive power variations where $\Delta V = -B^{-1}\Delta Q$ according to [24]. Without loss of generality, the equation would then be as follows:

$$[\Delta |V_u(k+1)|] = -[\Delta V_u(k)] - [B_{uu}]^{-1}[B_{uc}][\Delta |V_c(k)|] \tag{7}$$

In order to align with the common notation in the control theory field, we execute the following variable changes: $x(k) = \Delta V_u(k)$ and $\Delta V_c(k) = \mu(k)$. Thus, the previous equation can be expressed as:

$$x(k+1) = -x(k) - [B_{uu}]^{-1}[B_{uc}]\mu(k) \tag{8}$$

where $x(k)$, $\mu(k)$ are the vector of non-controllable variables and controller actions respectively.

4. Design of the proposed control

We propose the following predictive control problem: considering that it is necessary to minimize the deviation of the node voltages, the overall objective function is a linear quadratic function such as that presented in [25]. The main objective of the control is to keep the bus voltage magnitudes within the rated voltage limits at all times. In our analysis we consider this to be between 0.9 and 1.05 (pu). In the following equation, this objective is achieved by minimizing the voltage deviation of all grid nodes, including in the vector $x(k)$. The secondary objective is to minimize the action of the controllers and hence the operating cost of all controllers included in the vector $\mu(k)$. The optimal operation of the zones – e.g. minimization of active power losses or maximization of reactive power reserves – is not considered in this work as it is left to the TSOs. The timescale of short-term voltage control focused on in this paper is the period of several tens of seconds after a disturbance.

$$f(\cdot) = \sum_{k=0}^{N_p-1} x(k)^T * Q * x(k) + \mu(k)^T * R * \mu(k) \tag{9}$$

where N_p is the prediction horizon and Q and R are positive definite weighting matrices.

The restriction for this optimization problem is related to the model developed for the variable Eq. (8) as derived in the previous section, i.e.

$$x(k+1) = -x(k) - [B]\mu(k) \tag{10}$$

As analysed previously, using the sensitivity matrix and separating the controllable and non-controllable buses (the controllable buses are buses in which the compensators are connected), we have a decomposition problem. In the $[B] = [B_{uu}]^{-1}[B_{uc}]$ matrix, the concept of electrical distance is incorporated and therefore the effect of the voltages of the intermediate buses (from the controllers to the uncontrolled buses) is modelled. With this procedure it becomes necessary to separate the controls in the system dynamics model. This is a control problem with sharing buses, i.e. their actions affect buses in their areas of influence as well as common buses. This creates some complexity when adjusting the common interface as described in [26] and represented in Fig. 3. Usually the decomposition problems in power systems use fictitious buses. Our proposal focuses on buses between the compensators, called common buses. In this example, the decomposition of the system generates eight variables. The decomposition procedure is based on cloning the variables of the common buses. Each STATCOM has its own replica of the active and reactive power flows, voltage and phase angle deviation on bus 5. This bus is located on the line connecting STATCOM 1 and 2. These variables are known as consensus variables on which an iterative procedure is executed to reach a consensus. It is therefore possible to convert the network Fig. 3(a) in an equivalent (b) incorporating the variables of interest of each bus shared by the compensators.

As explained above, an ith controller has a set of buses in its neighbourhood on which it has a relevant impact, i.e. it alters their voltages. This neighbourhood is determined by the sensitivity $S = [B_{uu}]^{-1}[B_{uc}]$ defined previously. Within those buses there may be buses that are also controlled by another controller $'j'$. These buses are known as common buses, and a consensus between the i and j controllers is required for a proper control design so that the variables are equal. In the

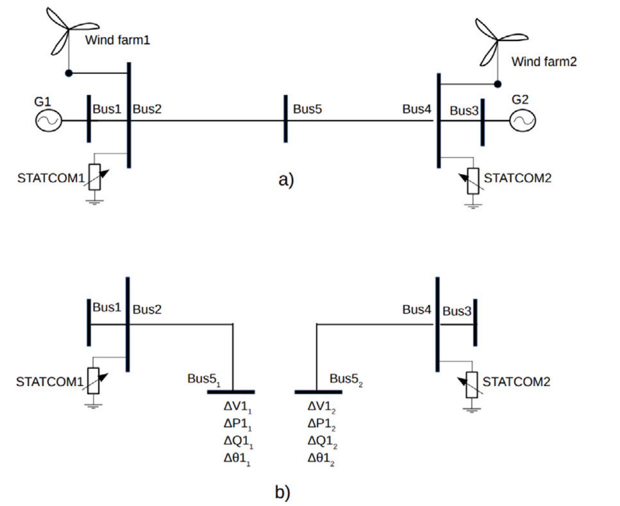

Fig. 3. Illustration of the proposed decomposition problem with a common bus.

decomposition process of the global model (11) this consensus appears as a restriction, which is incorporated into each controller applying the augmented Lagrangian with the condition of consensus at time step k as follows:

$$\min_{\mu_i} \sum_{i=1}^{n}\left(\sum_{l=0}^{N-1} x_i(k+1+l)^T * Q_i * x_i(k+1+l) + \mu_i(k+l)^T * R_i * u_i(k+l) + \sum_{j\in\Omega_i}\left(\lambda_{ji}(k)(Y_{ji}(k) - Y_{ij}(k)) + \frac{\gamma}{2}\left\|Y_{ji}(k) - Y_{ij}(k)\right\|^2\right)\right)$$

subject to:

$$\begin{aligned}
x_1(k+1+l) &= (-x_1(k+l)) - (B_1)(\mu_1(k+l))\text{v=20pt} - \sum_{j=1,j\neq 1}^{n_j} B_{j1}\mu_j(k+l) \\
x_2(k+1+l) &= (-x_2(k+l)) - (B_2)(\mu_2(k+l)) - \sum_{j=1,j\neq 2}^{n_j} B_{j2}\mu_j(k+l) \\
&\vdots \\
x_i(k+1+l) &= (-x_i(k+l)) - (B_i)(\mu_i(k+l)) - \sum_{j=1,j\neq i}^{n_j} B_{ji}\mu_j(k+l)
\end{aligned} \tag{11}$$

for $l = 0,\ldots,N-1$, $\lambda_{ji}(k)(Y_{ji}(k) - Y_{ij}(k))$ is the consensus term, $\frac{\gamma}{2}\left\|Y_{ji}(k) - Y_{ij}(k)\right\|^2$ is the penalization term and Ω_i is the set of neighbourhood controls of i. As can be observed, the objective function has the relaxed coupling constraint, and, in addition, a quadratic term is included to guarantee local convexity and improve convergence [25, 26].

The Lagrange multipliers weigh up the difference in the voltage values calculated by the local controllers. This helps the problem to converge. To linearize the proposed formulation in (11), the auxiliary problem principle is applied as in [27], so the local problem for control i, at time step k consists of:

$$\begin{aligned}
\min_{\mu_i} &\sum_{l=0}^{N-1} x_i(k+1+l)^T * Q_i * x_i(k+1+l) + \mu_i(k+l)^T * R_i * \mu_i(k+l) \\
&+ \sum_{j\in\Omega_i}\Big(\lambda_{ji}(k)^p Y_{ji}(k)^p + \frac{\beta}{2}\left\|Y_{ji}(k)^p - Y_{ji}(k)^{p-1}\right\|^2 \\
&+ \gamma Y_{ji}(k)^p(Y_{ji}(k)^{p-1} - Y_{ij}(k)^{p-1})\Big)
\end{aligned}$$

subject to:

$$x_i(k+1+l) = -x_i(k+l) - [B_i](\mu_i(k+l)) - \sum_{j=1,j\neq i}^{N_j}[B_j]\mu_j(k+l) \tag{12}$$

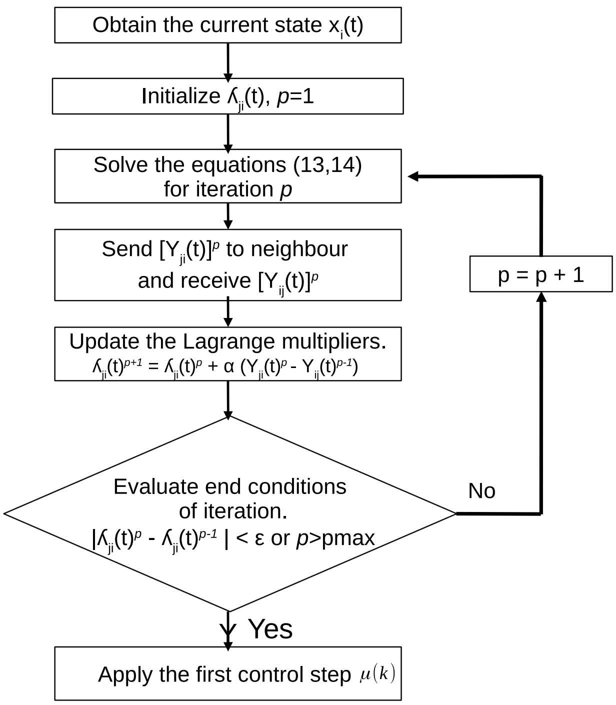

Fig. 4. Flowchart for the proposed DMPC local controller.

where: $\frac{\beta}{2}\left\|Y_{ji}(k)^p - Y_{ji}(k)^{p-1}\right\|^2 + \gamma Y_{ji}(k)^p (Y_{ji}(k)^{p-1} - Y_{ij}(k)^{p-1})$ are penalization terms.

For the update of the λ values, we use:

$$\lambda_{ji}(k)^{p+1} = \lambda_i(k)^p + \alpha(Y_{ji}(k)^p - Y_{ij}(k)^p) \tag{13}$$

Due to the interactions between the controls it is necessary to agree on their actions, therefore the controls must participate in a series of iterations. In each iteration p local calculations are performed, in which the value of the consensus variable $Y_{ij}(k)^{p-1}$ calculated by the neighbouring controls in the previous iteration is considered. In turn, the local control calculates $Y_{ji}(k)$ and publishes it.

The predictive control problem i proposed in this paper is formulated in Eq. (12). Here the vector x_i are the buses that belong to the area of influence (Ω_i) of the controller, Q_i, R_i are weighting matrix, λ_{ji} are the Lagrange multipliers associated with the consensus, and γ and β are positive constants. $[B_i]$ and $[B_j]$ are column vectors of sensitivity which relate the vector x_i states to control i or j, and the $\sum_{j=1,j\neq i}^{N_j}[B_j]\mu_j(k+l)$ term is referred to as the disturbance on the variable x_i generated by the actions of the neighbouring controls. Fig. 4 depicts the flowchart of the DMPC-based local controller.

5. Plug-and-play connection

One of the main advantage of our proposed algorithm relies on the fact that is simple to implement, even if the power system is already installed. Let us suppose a power system which contains N wind farms with their respective STATCOMs as support for the voltage control. To incorporate and execute the proposed DMPC in the bus i, we will need to go on the following steps:

- Determine the sensitivity from each bus i on which a farm is installed to other nodes j in the power system. This can be easily done, as the system operator usually knows the topology of the system and the parameters of the lines, and from these two data the susceptance matrix can be calculated and the sensitivity matrix S_{ji} can be obtained.
- Analyse these results to determine the set of nodes $k_i \subset j$ that make up the neighbourhood of each farm i.
- Identify the common nodes, which are those that are repeated in the previous set for different wind farms.
- Install metering on the set of nodes k_i in the neighbourhood.
- Install the proposed controller on the farm i. Identify in the controller program which nodes k_i belong to the neighbourhood of this controller. Then, identify in the controller of the set k_i which are common nodes and to which other controller it belongs. Connect the meter readings of the k_i nodes to the i controller.
- Connect the output of the proposed controller to the SP input of the STATCOM internal control.

As can be seen from the above listed steps, there is no information about the internal dynamics of the machines. Additionally, the controller can be installed in the desired number of wind farms but it is not necessary to install it in all of them.

Once a wind farm receives the setpoint by the proposed DMPC, the coordination among the wind turbines in this wind farm can be accomplished by other controllers as the ones in [7–9].

6. Evaluation and test results

To assess the effectiveness of the designed control, the algorithm is implemented in MATLAB with the YALMIP toolbox. This toolbox helps to model and resolve optimization problems [28]. In particular, we have initially tested the control in the IEEE 9-bus test system, illustrated in Fig. 5. For this network, bus 1 (B1) is a slack node, buses 2 and 3 (B2 and B3) are PV and buses 4, 5, 6, 7, 8 and 9 (B4, B5, B6, B7, B8 and B9) are PQ. In the power system, we have incorporated two wind farms and the two corresponding STATCOMs, which are effective voltage compensators [29]. As usual, STATCOMs have a shunt connection with a non-negligible line impedance so the power system also includes nodes 11 and 12 (B11 and B12 in the figure).

We have tested the performance of the power system with four different configurations: (i) no control applied to the wind farm buses; (ii) fixed set point (SP) for the STATCOMs of the wind farms, i.e. the same value is kept for any event; (iii) centralized control applied to the two STATCOMS; and (iv) proposed DMPC executed in these voltage compensators. The DMPC is executed every 200 ms and all the iterations must be done in this interval.

For the controller we propose, we need to calculate the sensitivity of the grid nodes with respect to the nodes with a POC. This matrix helps to determine the buses that have the highest sensitivity to voltage changes in the POCs and those that are common to the controllers. When the value of the sensitivity in a node with respect to a POC is above a certain value, it is considered to be a node in the neighbourhood of that controller, and if it is also within the neighbourhood of another controller then it is said to be a node common to both controllers. As explained in the previous section, in this case the node will be considered a consensus node for our distributed algorithm. Table 2 represents the sensitivity that all nodes have with respect to the controllers in points of connection POC11 and POC12. For POC 11, buses 1, 4, 5 and 9 have the highest sensitivity values so that these buses can be considered in the vicinity of bus 11. For POC 12, the same analysis is carried out, concluding that nodes 2, 3, 6, 7, 8 and 9 are in the vicinity of bus 12. It can be observed that bus 9 belongs to both vicinities, i.e. bus 9 is a common bus that requires a consensus in our algorithm.

We have changed the reactive load in the PQ buses B5 and B7. At the beginning of the simulation, the load in bus B5 is 90 MW and 30 MVAr. In bus B7, the load is 100 MW and 35 MVAr; while in bus B9 we have initially set 125 MW and 50 MVAr. Then, at 0.5 s the inductive power on bus B5 is increased by 20 MVAr. At 0.8 s, the load on bus B7 is incremented by 50 MVAr, leading to a total reactive of 185 MVAr

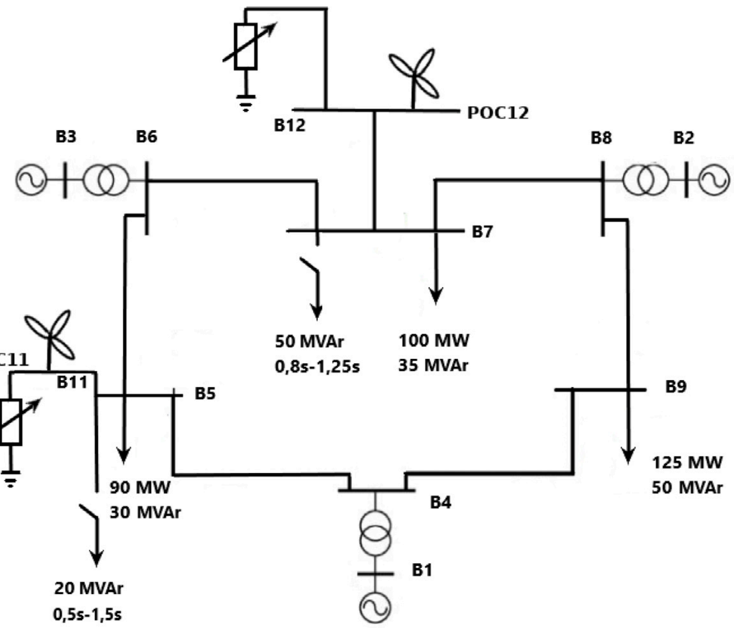

Fig. 5. Diagram of IEEE-9 bus test system with two wind farms and their corresponding STATCOMs.

Table 2
Sensitivity matrix.

Bus	POC	
	11	12
1	**0.7410**	0.3075
2	0.2636	**0.7797**
3	0.4098	**0.6273**
4	**0.7410**	0.3075
5	**0.8995**	0.1182
6	0.4098	**0.6273**
7	0.1182	**0.8999**
8	0.2636	**0.7797**
9	**0.5868**	**0.4745**

Table 4
Maximum number of iterations for convergence of the DMPC.

N	Configuration			
	β	γ	α	I_{max}
3	2	1	0.1	5
7	10	0.1	0.1	5
30	2	1	0.1	5
3	2	1	1	15
7	2	0.1	1	15
7	0.1	2	1	15
30	2	0.1	1	15
7	0.1	0.1	10	30
7	2	1	10	30

Table 3
PF resolution in the PV nodes for the analysed configuration of the IEEE-9 bus test system for the initial load conditions.

Bus	B1	B2	B3
Type	Swing	PV	PV
P [MW]	72	85	163
Q [MVAr]	42	−2	−7.4

and active 235 MW. Later, at 1.2 s the 50 MVAr are removed from bus B7 and at 1.5 s the 20 MVAr are removed from bus B5.

For the initial load, we can determine the system parameters. With an PF algorithm, we obtain the powers specified in Table 3. Since the goal of our algorithm is for the load variations to be compensated by the STATCOMs connected to the wind farms, it will be easy to see the power contributions of the compensators on these initial values when evaluating the simulation results.

The influence of the parameters on the algorithm was studied by running several simulations with different values of these parameters and constructing Table 4. The control interval of the DMPC was set at t = 0.2 s and the load variations described previously at t = 0.5 s, 0.8 s, 1.2 s and 1.5 s. It should be pointed out that the maximum number of iterations (I_{max}) is affected mostly by α, and to a lesser degree by β. The impact of γ is less significant, so it is not specified for any configuration. Decreasing any of these parameters causes the number of iterations to decrease and therefore decreases the control execution time. Each step of the prediction horizon is equal to the control interval and should cover the transient response of the open-loop system. Although a very long N should lead to a more stable performance, it also implies a great computational effort. Nevertheless, this assumption does not always hold. In fact, in [30] we demonstrate how a low N in many electrical systems gives the same results as a long one. The most commonly used method to determine the optimal N value is trial and error. From the simulation results shown in Table 4, the same response is obtained from N = 3 to 30, therefore N = 3 was chosen.

An empirical procedure was used with a constant step size, $\alpha = \beta/2 = \gamma$. $alpha$ and $gamma$ are constants that weigh up the difference of the negotiation variables so they can be equalized. Then, a step size of $alpha = 1$ was chosen, since – as obtained from the simulations – this value gives a low number of iterations for convergence. Finally the chosen values are $N = 3$, $\alpha = 1$, $\beta = 2$ and $\gamma = 1$. For this configuration, we have analysed some metrics. In Fig. 6, we show the deviation of the voltages from the desired value (1 (pu)) in the load buses for each control technique evaluated. It immediately stands out that the proposed control is very similar to the centralized control and that it also reduces the number of oscillations with respect to the fixed control when there are load changes. For this reason, it is interesting to test the deviation with respect to the centralized control in the further analysis.

In Fig. 7, we show the deviation with respect to values derived by the centralized control. Highlighting and as mentioned above if no control is applied, the system suffers from a high variability of the voltage levels. If used with a fixed set point value, peaks appear at

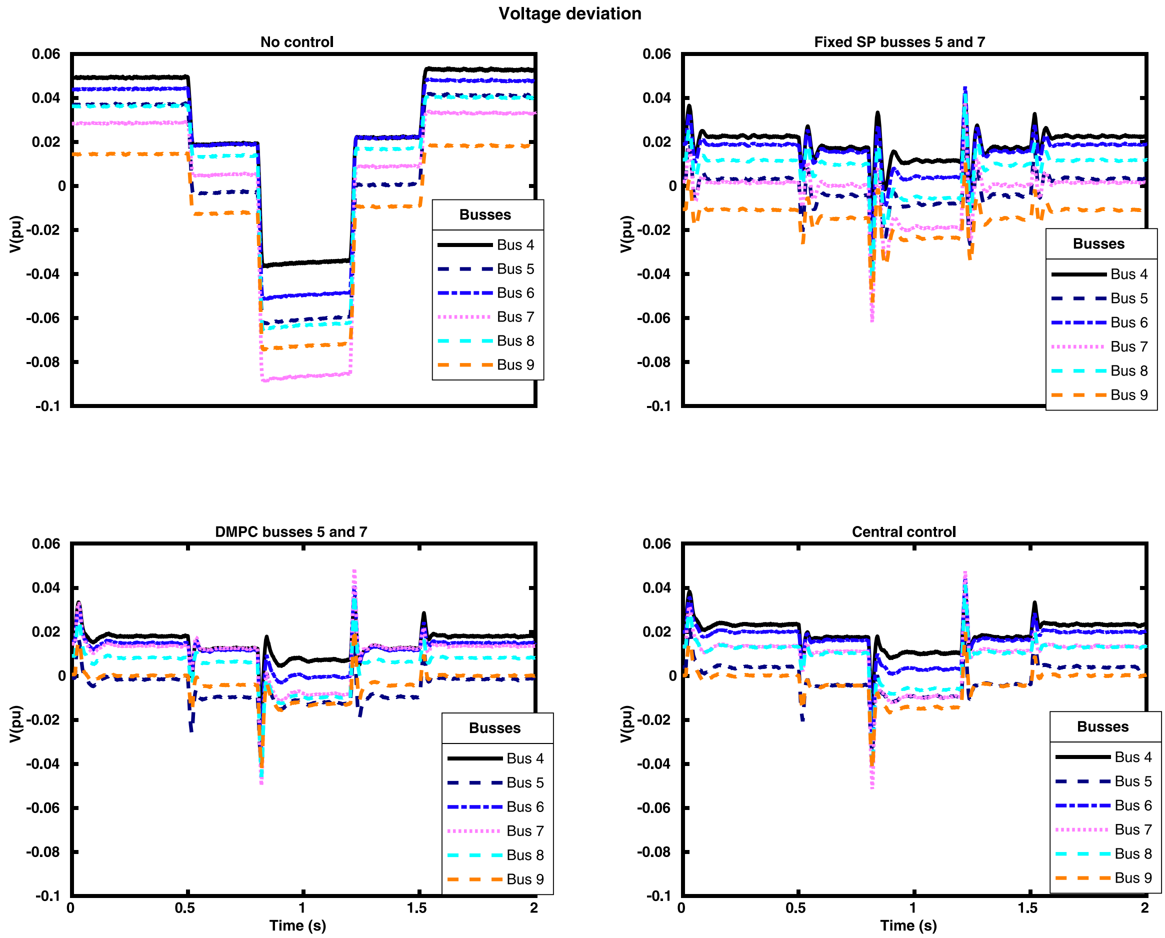

Fig. 6. Deviation of the bus voltage values in IEEE 9-bus test system.

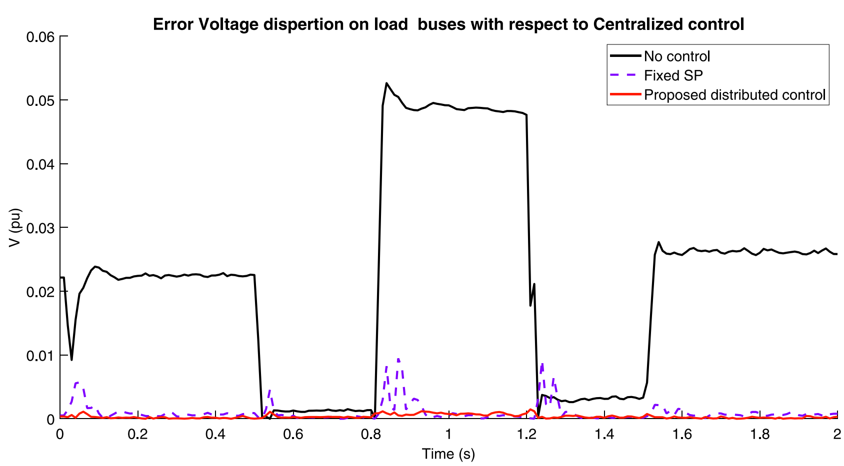

Fig. 7. Voltage dispersion for every control algorithm compared to the centralized solution in IEEE 9-bus test system.

changes in the system load, showing an error with respect to centralized control, whereas the proposed distributed control generates very similar dynamics to the centralized control. We can see that the oscillations are minimized with the DMPC algorithm. In order to assess the convergence of the λs coefficients, we have analysed the updates of this parameter during the iterations. Fig. 8 represent this evolution for the first execution of the DMPC algorithm. The Lagrange multiplier updating schemes in Eq. (13) is based on the calculation of sub-differentials. This scheme is well-known to suffer from oscillatory behaviour as it is shown in Fig. 8. However, it can be observed that the values tend to a stable number for all the iterations. It can be seen that there is a positive λ value and a negative one. The λs are used to establish how and in what sense each controller approaches the solution or the desired value of the consensus variable. Therefore, λs reflect how fast a solution is sought and this is set by the α coefficient. Regarding the direction in which the solution is defined, the difference of the values of the consensus variable calculated in each iteration is an indicator of this movement. In one control, we have $\alpha * (Y1 - Y2)$ and in the another we have specified $\alpha * (Y2 - Y1)$. This configuration forces each control to approach the final solution in opposite directions.

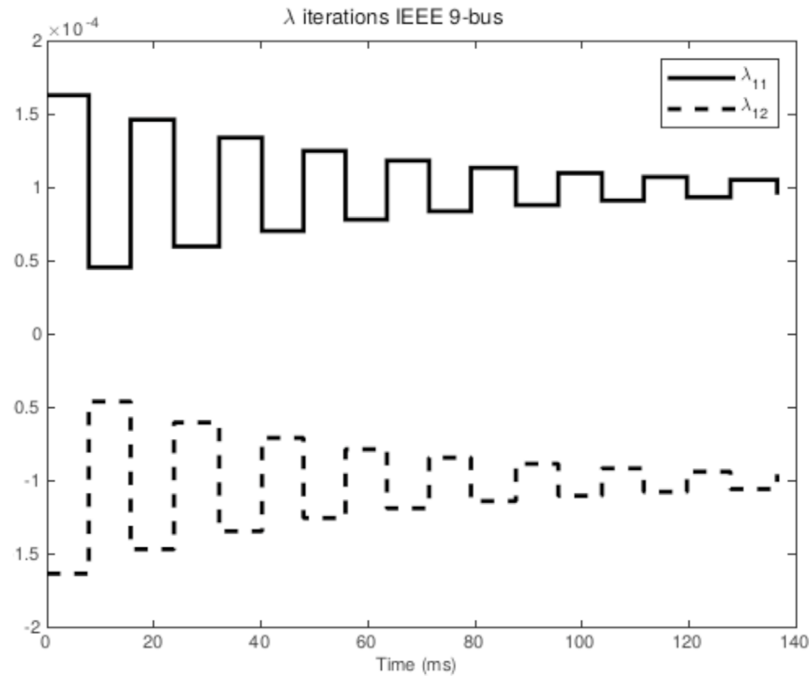

Fig. 8. Convergence of the λ coefficients for the first execution in the in IEEE 9-bus test system.

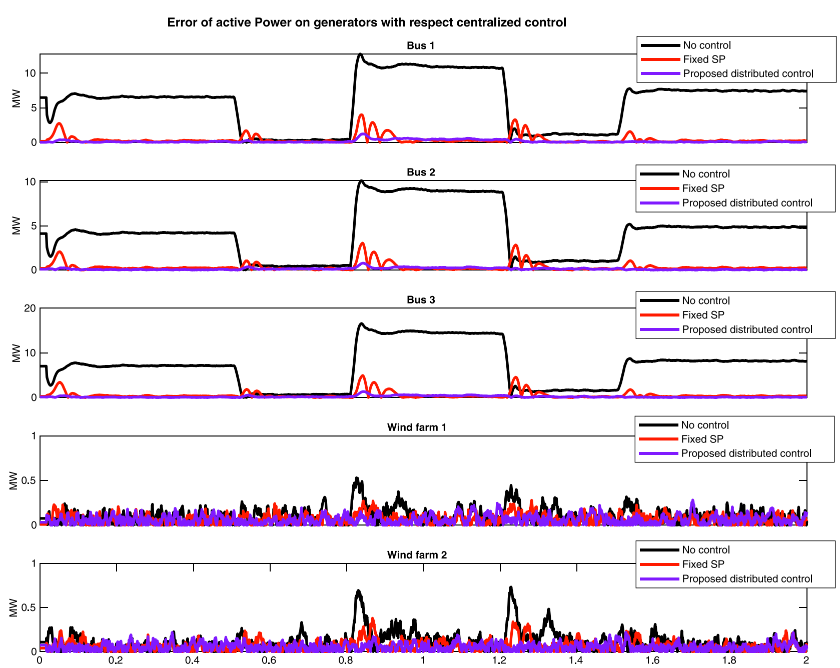

Fig. 9. Active power on generation buses for every control technique in IEEE 9-bus test system.

A similar performance is observed for other changes on the load. To evaluate the performance of the DMPC code, the execution time of the algorithm was measured using the tic and toc functions provided by Matlab. A Dell Inspiron 15 laptop machine was used. It is an Intel© Core™ i7-8550U CPU @ 1.80 GHz × 4, 8 GB memory and it runs Linux Mint 19.3 Cinnamon. We got a maximum value of 140 ms per execution of the DMPC algorithm. The execution of the DMPC algorithm includes several iterations until the convergence is achieved. Thus, by the execution time of the DMPC algorithm we mean the sum of time required by all the corresponding iterations to achieve convergence.

The next issue to evaluate is the support of the proposed control over the active and reactive power of the system generators. The previous resolution of the PF constitutes the reference for the operation of the IEEE 9-bus system. The support that the wind farms provide with the TSO restriction usually consists in keeping the generators at the power values calculated in the PF. With respect to the active power illustrated in Fig. 9, the simulation results show that both control strategies – the proposed DMPC and the centralized control – similarly support the generators during power variations, which validates the use of a distributed algorithm. A similar behaviour is observed for the reactive power in Fig. 10.

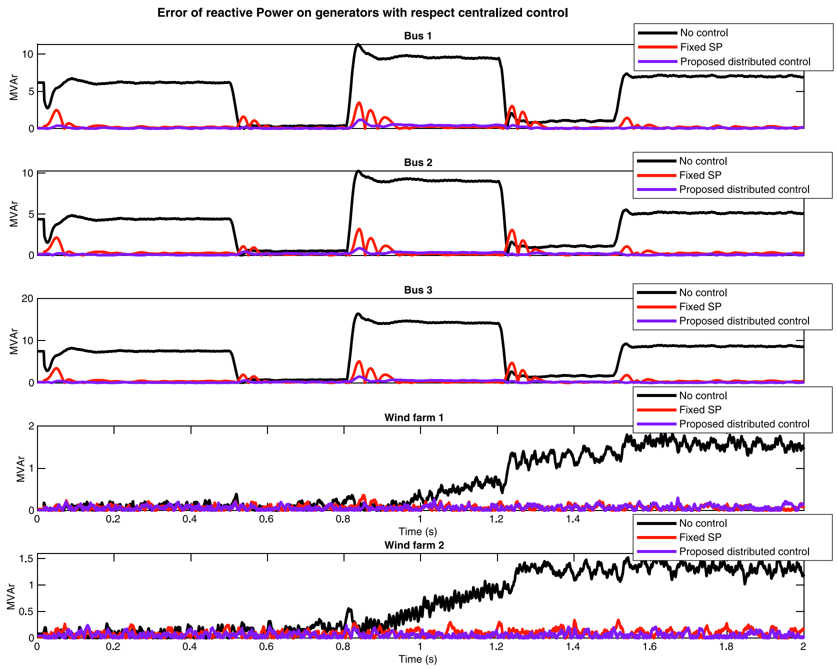

Fig. 10. Reactive power on the generation buses and on the wind farms in IEEE 9-bus test system.

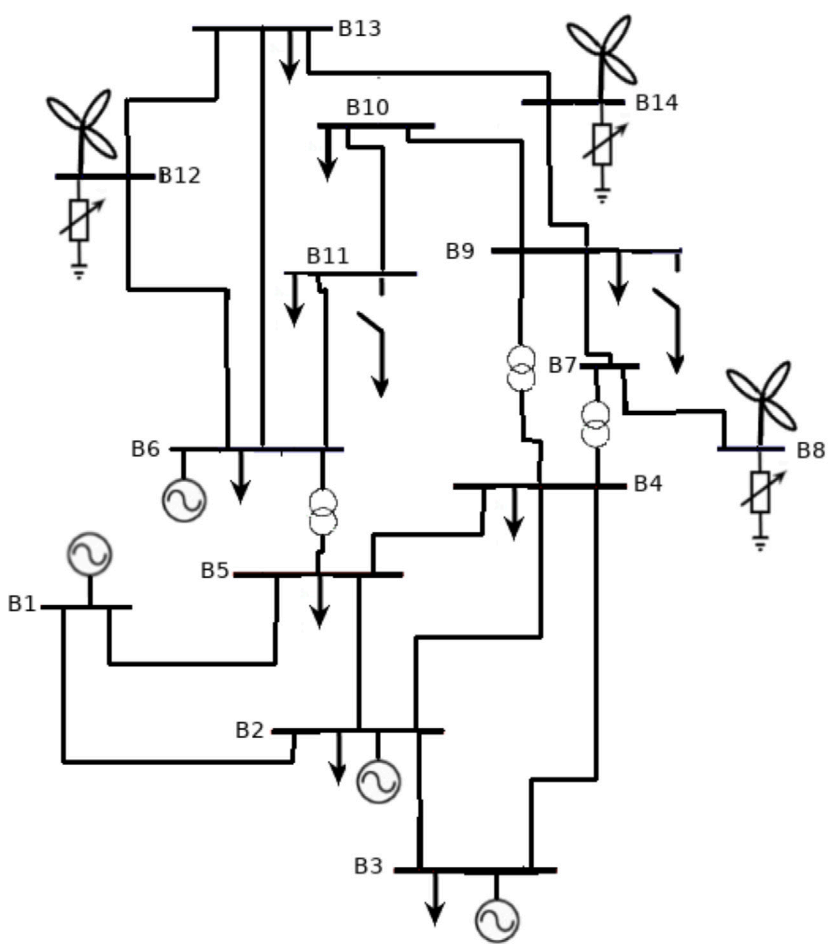

Fig. 11. IEEE-14 bus test system.

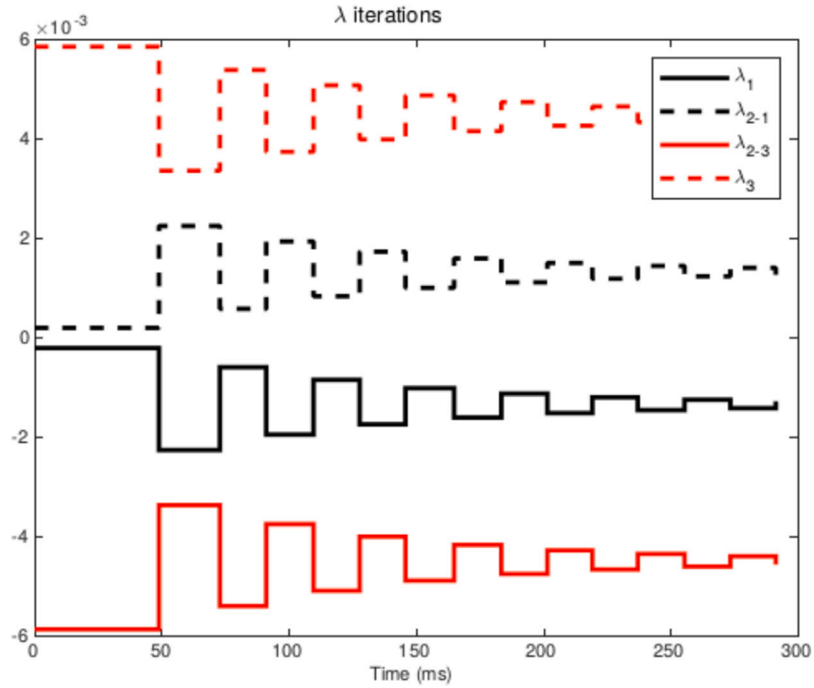

Fig. 12. λ values for the IEEE 14-bus test system.

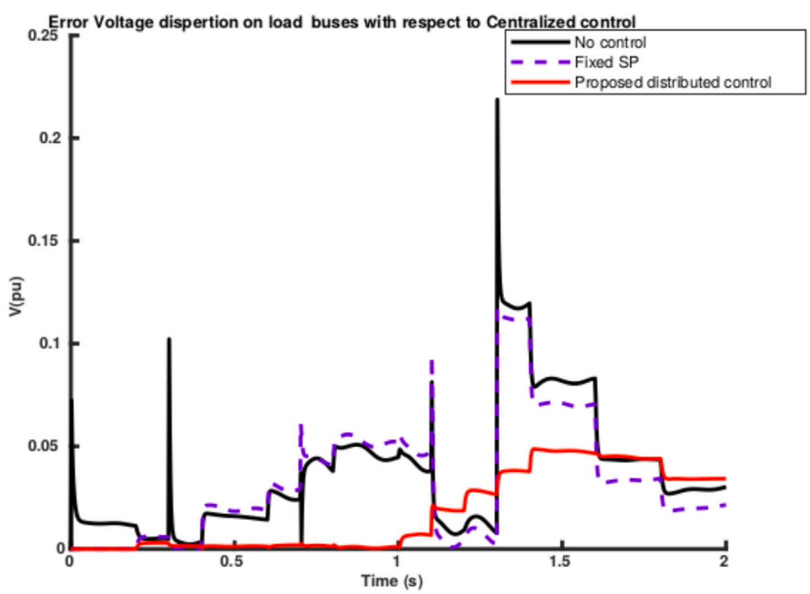

Fig. 13. Error of the voltage dispersion for every control algorithm in the IEEE 14-bus test system.

To evaluate the scalability of our proposal, we have also tested our algorithm on the IEEE-14 bus test system, illustrated in Fig. 11. It has been modified with 3 wind farms with their respective STATCOMS installed on buses B8, B12 and B14 and 4 generators. For the WFs connected on buses B8 and B12, the common bus is B13 and for those on B12 and B14, it is B9. The reactive power of the bus B11 in $t = 0.3$ s was increased from 2.52 MVAR to 50 MVAR and in bus B9, we have set a change from 23.24 MVAR to 60 MVAR at $t = 0.7$ s. Then in $t = 1.1$ s and 1.3 s they return to their initial powers respectively.

With two common buses, 4 λ values are generated, two for each common bus. These lambdas are represented in Fig. 12 and as can be seen they converge on a time scale similar to that of the previous system. The λ_1 and λ_{2-1} are used for consensus between control 1 and control 2. Likewise the λ_3 and λ_{2-3} are used for the consensus between control 3 and control 2. Regarding the voltage dispersion, we can check that the proposed distributed approach approximates to the centralized solution better than when a fixed SP is applied. Fig. 13 shows these differences.

As can be seen in Fig. 12, the time to respond of each control is longer than the previous test system, because it increased the number of controls in consensus, as well as the number of buses that the controllers must consider i.e. the buses in the vicinity of each controller, which are affected by the controls according to the sensitivity. To further test the proposed control as shown in 13 the reactive power changes were made shorter in time. For example; there is a change from 1.1 to 1.3 s which are 200 ms and the control requires about 300 ms, so in this time span the controls fail to correct the voltage profiles. However after 1.1 s it can be seen how the control is improving the response thanks to the closed loop effect that generates the prediction horizon which finally gives stability to the system.

7. Conclusions

In this article, we propose a DMPC for voltage compensators with the goal of locally generating the reference signal or control setpoint. Our proposal uses information regarding the most influencing nodes (identified with the electrical distance). In fact, the controller was designed based on the sensitivity values (Jacobian matrix), which guarantees that the network topology is intrinsically included in the algorithm. This helps to determine the area of influence on the controller. Since it does not require any structural variables of the compensator controls in the design, the proposal can be considered a plug-and-play scheme. The interaction with neighbouring distributed controls are considered through the consensus of common buses. This locally generates the reference signal or setpoint of the compensator controller from this consensus. The algorithm was tested through two power systems with two and three large-scale wind farm units in a transmission network respectively. The tests validated the fact that the control considerably reduces the deviation of the bus voltage values. The simulation output shows that the proposed distributed approach approximates correctly to the results obtained by the centralized control in both scenarios. The scalability of the solution has also been validated.

This control can be applied to any voltage compensator device or machine with a local voltage control when it has an accessible input for the setpoint. The algorithm is able to cope with variations in the topology or the load profile. This capability is due to the fact that the formulation of the algorithm relies on the electrical distance or sensitivity matrix and therefore the network topology is considered intrinsically.

CRediT authorship contribution statement

César Contreras: Conceptualization, Methodology, Software, Writing – original draft, Writing – review & editing. **Alicia Triviño:** Formal analysis, Data curation, Visualization, Writing – original draft, Writing – review & editing. **José A. Aguado:** Methodology, Formal analysis, Writing – review & editing, Supervision.

Declaration of competing interest

The authors declare that they have no known competing financial interests or personal relationships that could have appeared to influence the work reported in this paper.

Acknowledgements

This work has been partially funded by the Spanish Ministerio de Ciencia e Innovacion (MICINN) by project PID2019-110531-RA-I00 from the "Proyectos de I+D+i - RTI Tipo A" programme and by the Consejería de Transformación Económica, Industria, Conocimiento *y* Universidades (Junta de Andalucía), Spain through project P20-01164. The research network RIEMOV "Red Iberoamericana de Investigación en Electromovilidad', which was founded by Asociación Universitaria Iberoamericana de Postgrado (AUIP), has promoted the collaboration of the authors.

References

[1] Wiser RH, Bolinger M. 2018 wind technologies market report. 2019, http://dx.doi.org/10.2172/1559241, https://www.osti.gov/biblio/1559241.
[2] Guo Y, Gao H, Wu Q. Distributed cooperative voltage control of wind farms based on consensus protocol. Int J Electr Power Energy Syst 2019;104:593–602. http://dx.doi.org/10.1016/J.IJEPES.2018.07.030.
[3] Li Q, Zhang Y, Ji T, Lin X, Cai Z. Volt/var control for power grids with connections of large-scale wind farms: A review. IEEE Access 2018;6:26675–92. http://dx.doi.org/10.1109/ACCESS.2018.2832175.
[4] Darabian M, Jalilvand A. Improving power system stability in the presence of wind farms using STATCOM and predictive control strategy. IET Renew Power Gener 2018;12. http://dx.doi.org/10.1049/iet-rpg.2016.0812.
[5] Guo Y, Gao H, Wu Q. Distributed cooperative voltage control of wind farms based on consensus protocol. Int J Electr Power Energy Syst 2019;104:593–602. http://dx.doi.org/10.1016/J.IJEPES.2018.07.030.
[6] Sun H, Guo Q, Qi J, Ajjarapu V, Bravo R, Chow J, Li Z, Moghe R, Nasr-Azadani E, Tamrakar U, Taranto GN, Tonkoski R, Valverde G, Wu Q, Yang G. Review of challenges and research opportunities for voltage control in smart grids. IEEE Trans Power Syst 2019;34(4):2790–801. http://dx.doi.org/10.1109/TPWRS.2019.2897948.
[7] Huang S, Wu Q, Guo Y, Lin Z. Bi-level decentralized active and reactive power control for large-scale wind farm cluster. Int J Electr Power Energy Syst 2019;111:201–15. http://dx.doi.org/10.1016/j.ijepes.2019.03.045.
[8] Tan H, Li H, Yao R, Zhou Z, Liu R, Wang X, Zheng J. Reactive-voltage coordinated control of offshore wind farm considering multiple optimization objectives. Int J Electr Power Energy Syst 2022;136:107602. http://dx.doi.org/10.1016/j.ijepes.2021.107602.
[9] Jiao W, Wu Q, Huang S, Chen J. Decentralized voltage control of wind farm based on gradient projection method. Int J Electr Power Energy Syst 2020;123:106308. http://dx.doi.org/10.1016/j.ijepes.2020.106308.
[10] Moradzadeh M, Boel R, Vandevelde L. Voltage coordination in multi-area power systems via distributed model predictive control. IEEE Trans Power Syst 2013;28(1):513–21. http://dx.doi.org/10.1109/TPWRS.2012.2197028.
[11] Khazaei J, Amini MH. Protection of large-scale smart grids against false data injection cyberattacks leading to blackouts. Int J Crit Infrastruct Prot 2021;35:100457. http://dx.doi.org/10.1016/j.ijcip.2021.100457.
[12] Antoniadou-Plytaria KE, Kouveliotis-Lysikatos IN, Georgilakis PS, Hatziargyriou ND. Distributed and decentralized voltage control of smart distribution networks: Models, methods, and future research. IEEE Trans Smart Grid 2017;8(6):2999–3008. http://dx.doi.org/10.1109/TSG.2017.2679238.
[13] Guo Y, Gao H, Wu Q, Østergaard J, Yu D, Shahidehpour M. Distributed coordinated active and reactive power control of wind farms based on model predictive control. Int J Electr Power Energy Syst 2019;104. http://dx.doi.org/10.1016/j.ijepes.2018.06.043.
[14] Lou G, Gu W, Xu Y, Cheng M, Liu W. Distributed MPC-based secondary voltage control scheme for autonomous droop-controlled microgrids. IEEE Trans Sustain Energy 2017;8(2):792–804. http://dx.doi.org/10.1109/TSTE.2016.2620283.
[15] Guo Y, Wu Q, Gao H, Chen X, Ostergaard J, Xin H. MPC-based coordinated voltage regulation for distribution networks with distributed generation and energy storage system. IEEE Trans Sustain Energy 2019;10(4):1731–9. http://dx.doi.org/10.1109/TSTE.2018.2869932.
[16] Tang Z, Hill DJ, Liu T. Coordinated voltage control of weak sub-transmission networks considering wind power variability. IFAC-PapersOnLine 2015;48. http://dx.doi.org/10.1016/j.ifacol.2015.12.344.
[17] Liu B, Zhang X, Kong D, Liu X, Chang X. Research on reactive power and voltage coordination control strategy for multi-wind farm connecting to power grid. In: 2019 IEEE innovative smart grid technologies - Asia (ISGT Asia). IEEE; 2019, p. 1633–7.
[18] Musleh AS, Muyeen SM, Al-Durra A, Kamwa I. Testing and validation of wide-area control of STATCOM using real-time digital simulator with hybrid HIL-SIL configuration. IET Gener Transm Distrib 2017;11. http://dx.doi.org/10.1049/iet-gtd.2016.1557.
[19] Musleh AS, Muyeen SM, Al-Durra A, Khalid HM. PMU based wide area voltage control of smart grid: A real time implementation approach. In: 2016 IEEE innovative smart grid technologies - Asia (ISGT-Asia). 2016, p. 365–70. http://dx.doi.org/10.1109/ISGT-Asia.2016.7796413.
[20] Zheng T, Jiao S, Ding K, Lin L. A coordinated voltage control strategy of wind farms based on sensitivity method. In: 2013 IEEE Grenoble conference. 2013, p. 1–5. http://dx.doi.org/10.1109/PTC.2013.6652207.
[21] Lee HI, Bae M, Lee B. Advanced reactive power reserve management scheme to enhance LVRT Capability. Energies 2017;10. http://dx.doi.org/10.3390/en10101540.
[22] Faria WR, De Oliveira ME, Hoji ES, Viajante GP. Voltage control areas in transmission systems with distributed generation. Renew Energy Power Qual J 2017;1. http://dx.doi.org/10.24084/repqj15.332.
[23] Maestre JM, Negenborn RR. Distributed model predictive control made easy, Vol. 69. Dordrecht: Springer; 2014, http://dx.doi.org/10.1007/978-94-007-7006-5.
[24] Bidgoli HS, Van Cutsem T. Combined local and centralized voltage control in active distribution networks. IEEE Trans Power Syst 2018;33. http://dx.doi.org/10.1109/TPWRS.2017.2716407.
[25] Negenborn R, Netherlands Research School for Transport, Infrastructure and Logistics. Multi-agent model predictive control with applications to power networks. TRAIL thesis series, Netherlands TRAIL Research School; 2007, URL https://books.google.co.ve/books?id=4wtRMQAACAAJ.
[26] Arnold M, Knopfli S, Andersson G. Improvement of OPF decomposition methods applied to multi-area power systems. In: 2007 IEEE Lausanne power tech. 2007, p. 1308–13. http://dx.doi.org/10.1109/PCT.2007.4538505.

[27] Christofides PD, Scattolini R, Muñoz de la Peña D, Liu J. Distributed model predictive control: A tutorial review and future research directions. Comput Chem Eng 2013;51. http://dx.doi.org/10.1016/j.compchemeng.2012.05.011.
[28] Ravat AK, Dhawan A, Tiwari M. LMI and YALMIP: Modeling and optimization toolbox in MATLAB. In: Lecture notes in electrical engineering, Vol. 683. Springer Science and Business Media Deutschland GmbH; 2021, p. 507–15.
[29] Pathak AK, Sharma MP, Bundele M. A critical review of voltage and reactive power management of wind farms. Renew Sustain Energy Rev 2015;51:460–71. http://dx.doi.org/10.1016/J.RSER.2015.06.015.
[30] Sawma J, Khatounian F, Monmasson E, Ghosn R, Idkhajine L. The effect of prediction horizons in MPC for first order linear systems. In: IEEE international conference on industrial technology (ICIT). 2018, p. 316–21. http://dx.doi.org/10.1109/ICIT.2018.8352196.